Received: 1 May 2024 | Revised: 4 September 2024 | Accepted: 5 September 2024

DOI: 10.1002/alz.14297

Alzheimer's & Dementia®
THE JOURNAL OF THE ALZHEIMER'S ASSOCIATION

RESEARCH ARTICLE

The Taiwan-ADNI workflow toward integrating plasma p-tau217 into prediction models for the risk of Alzheimer's disease and tau burden

Kuo-Lun Huang[1] | **Ing-Tsung Hsiao**[2,3] | **Chi-Wei Huang**[4] | **Chung-Guei Huang**[5] | **Hsin-I Chang**[4] | **Shu-Hua Huang**[6] | **Kun-Ju Lin**[3] | **Mi-Chia Ma**[7] | **Chin-Chang Huang**[1] | **Chiung-Chih Chang**[4,8]

[1]Department of Neurology, Linkou Chang Gung Memorial Hospital, Chang Gung University, Taoyuan, Taiwan

[2]Department of Medical Imaging and Radiological Sciences and Healthy Aging Research Center, Chang Gung University, Taoyuan, Taiwan

[3]Department of Nuclear Medicine, Linkou Chang Gung Memorial Hospital, Chang Gung University, Taoyuan, Taiwan

[4]Department of Neurology, Cognition and Aging Center, Institute for Translational Research in Biomedicine, Kaohsiung Chang Gung Memorial Hospital, Chang Gung University College of Medicine, Kaohsiung City, Taiwan

[5]Department of Medical Laboratory, Linkou Chang Gung Memorial Hospital, Department of Medical Biotechnology and Laboratory Science, Chang Gung University, Taoyuan, Taiwan

[6]Department of Nuclear Medicine, Kaohsiung Chang Gung Memorial Hospital, Chang Gung University College of Medicine, Kaohsiung City, Taiwan

[7]Department of Statistics, College of Management, National Cheng Kung University, Tainan, Taiwan

[8]School of Medicine, College of Medicine, National Sun Yat-sen University, Kaohsiung, Taiwan

Correspondence
Chiung-Chih Chang, Department of Neurology, Cognition and Aging Center, Institute for Translational Research in Biomedicine, Kaohsiung Chang Gung Memorial Hospital, Chang Gung University College of Medicine, No. 123 Ta-Pei Rd, Niau-Sung Dist., Kaohsiung City 833401, Taiwan.
Email: neur099@cgmh.org.tw

Funding information
National Science and Technology Council, Grant/Award Numbers: NSTC112-2321-B-182A-004, NSTC112-2314-B-182-053, NSTC113-2314-B-182-042-MY2, NSTC113-2321-B-182A-005, NSTC110-2314-B-182A-073-MY3; Chang Gung Memorial Hospital, Grant/Award Numbers: CORPG8N0041, CMRPG8J0524, CMRPG8J0843, CMRPG3P0861, CMRPD1N0401, BMRP-488, CMRPG8K1533

Abstract

INTRODUCTION: We integrated plasma biomarkers from the Taiwan Alzheimer's Disease Neuroimaging Initiative and propose a workflow to identify individuals showing amyloid-positive positron emission tomography (PET) with low/intermediate tau burden based on [18F]Florzolotau PET-based quantification.

METHODS: We assessed 361 participants across the Alzheimer's disease (AD) and non-AD continuum and measured plasma phosphorylated tau (p-tau)217, p-tau181, amyloid beta (Aβ)42/40 ratio, neurofilament light chain, and glial fibrillary acidic protein levels at two medical centers. We evaluated the diagnostic potential of these biomarkers.

RESULTS: Among all plasma biomarkers, p-tau217 had the highest consistency with amyloid PET results (area under the curve = 0.94), and a cutoff value could have reduced the number of confirmatory amyloid PET scans by 57.5%. In amyloid PET–positive cases intending to use anti-amyloid therapy, p-tau217 level, along with clinical parameters, had the highest predictive ability for low/intermediate tau burden.

Kuo-Lun Huang and Ing-Tsung Hsiao contributed equally to this study.

This is an open access article under the terms of the Creative Commons Attribution-NonCommercial License, which permits use, distribution and reproduction in any medium, provided the original work is properly cited and is not used for commercial purposes.
© 2025 The Author(s). *Alzheimer's & Dementia* published by Wiley Periodicals LLC on behalf of Alzheimer's Association.

DISCUSSION: A two-step workflow based on p-tau217 and confirmatory amyloid PET could accurately classify AD patients showing low/intermediate tau burden.

KEYWORDS
[18F]Florzolotau positron emission tomography, Alzheimer's disease, amyloid positron emission tomography, low to intermediate tau burden, phosphorylated tau217

Highlights

- The emergence of anti-amyloid therapy increases the need to accurately diagnose Alzheimer's disease (AD).
- The use of plasma biomarkers, especially phosphorylated tau 217 (p-tau217), can help in the diagnosis of AD.
- P-tau217 is a better predictor of amyloid positron emission tomography (PET) positivity than other core biomarkers.
- In amyloid PET–positive individuals, p-tau217 can predict tau burden.
- We propose a two-step workflow to identify AD cases suitable for treatment.

1 | BACKGROUND

Alzheimer's disease (AD) is a common neurodegenerative disorder showing amyloid and tau pathology.[1] In 2023, lecanemab received traditional approval from the US Food and Drug Administration as a disease-modifying drug for AD (https://www.fda.gov/news-events/press-announcements/fda-converts-novel-alzheimers-disease-treatment-traditional-approval), while donanemab has shown promise in slowing clinical progression.[2] In these treatment trials, biomarker analyses other than amyloid positron emission tomography (PET) were also used to assess the drug effects, including tau PET and blood-based biomarkers. Analysis of tau PET after donanemab treatment supports that therapy targeting amyloid beta (Aβ) may eliminate downstream tau pathology,[3] especially in those showing low/medium tau pathology. Recent advances in plasma biomarkers have shown promise in predicting amyloid positivity, and use of the plasma biomarker phosphorylated tau 217 (p-tau217) as a screening tool for identifying individuals with amyloid positivity has been proposed.[3–6] Other AD-related plasma biomarkers including Aβ42/40, p-tau181, neurofilament light chain (NfL), and glial fibrillary acid protein (GFAP) have also shown clinical significance.[7–9] To date, blood-based biomarker studies in Asian populations are still limited, and further validation is required for their use in AD risk stratification.

Amyloid and tau PET can be used to visualize and quantify AD pathology in vivo, but tau deposition is more closely related to disease severity and progression. Tauopathy is categorized into different clinical spectra, and the accumulation of tau can be classified as 3-repeat (3R) tau, 4-repeat (4R) tau, or a mixture of the two. Many tau PET ligands tend to recognize specific aggregates, and the second-generation tau tracer [18F]Florzolotau can potentially identify all tau aggregates.[10,11] While it may not be the perfect technique for assessing the full spectrum of tau pathology, PET imaging with a second-generation tau tracer such as [18F]Florzolotau is probably the most comprehensive and direct tau pathology recognition technique currently available[12,13] for progressive supranuclear palsy (PSP)[13] and AD.[14] The binding specificity of [18F]Florzolotau on paired helical and straight filaments has been shown using cryo-microscopy,[15] supporting that the cortical binding uptake patterns in patients with AD[14] may be related to tau pathology. Likewise, the in vivo reactivity of [18F]Florzolotau with tau inclusions has also been supported by neuropathological examinations of brains tissue from PSP patients who underwent PET scans.[11]

According to the updated National Institute on Aging–Alzheimer's Association (NIA-AA) Clinical Criteria, the biological stage of AD progression should be determined by both amyloid and tau status.[16] Amyloid status is commonly dichotomized into positive or negative (A+/A–) by using visual assessment or semi-quantitative methods (i.e., standardized uptake value ratio [SUVR], Centiloid).[17,18] However, the evaluation of tau status notably varies according to the approach, analyzed cohort, region, and purpose.[19] In previous studies, tau status has been categorized as either positive or negative (T+/T–) or stages based on Braak stage volumes of interest (VOIs).[20,21] Even though tau loading is directly related to cognitive measurements, recent studies have shown that AD patients with a lower tau burden are more likely to benefit from disease-modifying treatment than those with a higher tau burden.[2,22–24] In addition, a recent study published in 2023 classified tau status into three levels of tau loading by fitting a Gaussian mixture model on the SUVR histogram, and also showed that p-tau217 had good predictive ability.[22] Therefore, to achieve satisfactory results using amyloid-targeting therapy, information about amyloid and tau burden are both essential.

However, the high cost, invasiveness, and limited availability of PET and cerebrospinal fluid tests may restrict their use, and thus blood-based biomarkers could be a routine screening option to meet the

scalability required for clinical application.[25] The aim of this study was to explore the feasibility of using multiple blood-based biomarkers from the Taiwan Alzheimer's Disease Neuroimaging Initiative (Taiwan-ADNI, T-ADNI) for screening AD and tau burden, and design a workflow for AD risk stratification in Asian populations.

RESEARCH IN CONTEXT

1. **Systematic review**: By reviewing the literature in public databases and search engines, we identified the clinical need to integrate plasma biomarkers into the diagnostic workflow to identify patients with Alzheimer's disease (AD) suitable for disease-modifying therapy.
2. **Interpretation**: In patients with cognitive impairment, we found that an appropriate cutoff phosphorylated tau 217 (p-tau217) value had high sensitivity, specificity, and positive and negative predictive values in identifying amyloid beta–positive individuals, and it could have reduced the number of amyloid positron emission tomography (PET) scans by 57.5%. Combining demographic data with p-tau217 resulted in the highest positive predictive agreement of low/intermediate tau burden based on [18F]Florzolotau PET quantification.
3. **Future directions**: In memory clinics, the integration of plasma p-tau217 will increase the accuracy of an AD diagnosis, reduce the number of amyloid PET scans, and predict tau burden to enable optimal treatment stratification.

2 | METHODS

2.1 | Study design and participants

This study was conducted in accordance with the Declaration of Helsinki and was approved by the institutional review board of Chang Gung Memorial Hospital. The Taiwan-ADNI[26] prospectively enrolled cognitively unimpaired (CU) participants, participants with mild cognitive impairment (MCI), and participants with dementia from two independent sites. For northern Taiwan, individuals were referred from Chang Gung Memorial Hospital, Linkou, and those in southern Taiwan were referred from Kaohsiung Chang Gung Memorial Hospital.[27] For research purposes, we included patients with PSP in this study, as the tau repeats in PSP are mainly composed of 4R tau. In addition to T-ADNI participants who were > 55 years old according to ADNI inclusion criteria, we also included a small portion of participants between 45 and 55 years old. The inclusion of these patients was to understand the clinical utility of plasma biomarkers.

2.2 | Diagnostic workflow and group stratifications

The study enrolled 361 participants, including 254 from Kaohsiung and 107 from Linkou (Table S1 in supporting information). The inclusion criteria for the CU participants were an age > 45 years, no cognitive symptoms, and a Clinical Dementia Rating (CDR) score of 0. The inclusion criteria for the MCI patients were: (1) age > 45 years; (2) memory complaints corroborated by an informant; (3) objective memory impairment adjusted for age and education, as judged by a physician; (4) preserved general cognitive functioning, with a CDR score of 0.5 and Mini-Mental State Examination (MMSE) score of 24 to 30; and (5) not fulfilling the criteria for dementia according to the Diagnostics and Statistical Manual of Mental Disorders, 5th edition (DSM-V). The inclusion criteria for the dementia patients were: (1) age > 45 years, (2) major cognitive symptoms with significant impairment of daily life activities, (3) CDR score ≥ 0.5 and MMSE score < 24, and (4) fulfilling the dementia criteria according to the DSM-V. Most of the participants in this study followed the age inclusion criteria of ADNI (i.e., 55 to 90 years old). A small portion of participants with younger age range (45–55 years old) were also recruited, including CU (7/51, 14%), MCI (1/104, 1%), and dementia (3/163, 2%). As plasma biomarkers may be confounded by age and to balance the age effects in patients with PSP and AD, we included 15 cases with early onset AD (EOAD) with age of onset before 65 years old. A clinical diagnosis of PSP was based on the 2017 research criteria,[28] with positive [18F]Florzolotau PET results in the brainstem and subcortical nuclei areas and negative amyloid PET results.

Apolipoprotein E (*APOE*) ε4 status was determined by the presence of rs429358 and rs7412 polymorphisms. Participants carrying *APOE* ε4 genotypes (heterozygous or homozygous) were defined as *APOE* ε4 carriers. All participants underwent the MMSE, CDR, and CDR Sum of Boxes (CDR-SB) and were required to have a partner provide an independent evaluation of daily functioning.

The exclusion criteria for all participants were: (1) a systemic disease or organ failure of substantial severity; (2) current alcohol or substance misuse; (3) refusal to undergo cognitive evaluations; and (4) cognitive impairment due to other non-degenerative etiologies, such as stroke, brain tumor, significant head trauma, normal pressure hydrocephalus, epilepsy, or psychiatric disorders.

2.3 | Image biomarker acquisition and analysis

[18F]Florbetapir and [18F]Florzolotau tracers were prepared and synthesized at the cyclotron facility of Chang Gung Memorial Hospital. [18F]Florbetaben was prepared and synthesized at PET Pharm Biotech (http://www.petpharmbio.com/EN/news.html).

2.3.1 | T-ADNI-Linkou

For the PET scans, all subjects underwent a 20 minute [18F]Florzolotau scan at 90 minutes post-injection with an injection dose of 202.2 ± 14.1 MBq, and a 10 minute [18F]Florbetapir scan at 50 minutes post-injection with an injection dose of 364.9 ± 18.0 MBq. Both the Biograph mCT PET/CT system (Siemens Medical Solutions) and

Discovery MI PET/CT system (GE Medical Systems) were used for PET acquisitions. For the mCT PET/CT system, a 3D ordered-subset expectation maximization algorithm was used for image reconstruction with parameters of four iterations and 24 subsets. A Gaussian filter of 2 mm full width at half maximum and zoom = 3 was applied for post-smoothing. Scatter and random correction were also performed using the correction methods provided by the manufacturer. The reconstructed images had a matrix size of 400 × 400 × 109 and a voxel size of 1.02 × 1.02 × 2.03 mm3. For the Discovery MI PET/CT system, images were reconstructed using a VUEPointHD ViP algorithm of four iterations, 16 subsets, and with a matrix size of 128 × 128 × 71 and a voxel size of 2 × 2 × 2.79 mm3. The PET images were motion corrected and averaged into 20 minute static scans for later processing. 3D T1-weighted magnetization prepared rapid gradient echo was acquired for each subject on a 3-T Siemens Magnetom TIM Trio scanner (Siemens Medical Solutions) with scanning parameters of 256 slices, repeat time: 2000 ms, echo time: 2.84 ms, inversion time: 900 ms, flip angle: 9°, with a voxel size of 1.0 × 1.0 ×1.0 mm.

2.3.2 | T-ADNI-Kaohsiung

Amyloid scans were acquired after the injection of 296 ± 74 MBq of [F18]Florbetaben (at 90 minutes post-injection) or [18F]Florbetapir (at 50 minutes post-injection). The tau PET scans were acquired at 90 minutes post-injection with a dose of 185 ± 74 MBq of [18F]Florzolotau. PET images were acquired on a GE Discovery MI PET/CT scanner (GE HealthCare). PET image acquisition consisted of two 5 minute dynamic frames. The PET images were motion corrected and averaged into 10 minute static scans for later processing. 3D T1-weighted magnetization prepared rapid gradient echo was performed on a 3T Skyra scanner (Siemens) using the following parameters: 176 slices, repeat time: 2600 ms, echo time: 3.15 ms, inversion time: 1090 ms, flip angle: 13°, with a voxel size of 1.0 ×1.0 ×1.0 mm.

2.4 | Image processing

Because the PET images were acquired from different scanners and processing protocols, preprocessing for data standardization is necessary.[29] All PET images in this study were preprocessed with pre-optimized scanner-specific filters derived from a Hoffman phantom so that all amyloid and tau PET images from different scanners resulted in a matched resolution for further analysis.[30–32]

The multimodality program PMOD (version 4.2, PMOD Technologies Ltd.) was used for image processing and analysis. Individual magnetic resonance images were initially normalized into the Montreal Neurological Institute (MNI) space, in which the transformation matrix was then applied to the corresponding co-registered PET images. Intensity normalization was then performed to compute the SUVR by using the inferior cerebellar cortex (crus) and whole cerebellum as reference regions for tau and amyloid PET, respectively. The automated anatomic labeling (AAL) atlas was modified and merged to obtain regional SUVR including the medial temporal lobe, lateral temporal lobe, parahippocampus, amygdala, frontal lobe, parietal lobe, anterior cingulate, posterior cingulate, precuneus, and occipital lobe for subsequent analysis. The entorhinal cortex was extracted from the Desikan–Killiany atlas.

2.5 | Biological diagnosis based on amyloid and tau PET

The biological status of amyloid and tau positivity was based on the PET results. Both amyloid and tau positivity were defined using visual reading evaluated by experienced nuclear medicine specialists according to the visual assessment criteria for [F18]Florbetapir,[33] [F18]Florbetaben,[34] and [18F]Florzolotau,[32] and further supported by the quantitative cutoff values (Supplementary Methods and Results in supporting information). Subjects with a visual reading score of 0 to 1 were assigned as being negative, and those with 2 to 4 scores as being positive.

All 361 individuals had amyloid visual reading scores, and 322 (89.2%) individuals completed tau PET. Accordingly, AD was defined as A+T+ (n = 114), in agreement with the updated NIA-AA 2018 criteria[35] and International Working Group 2 2021 criteria.[36] We stratified the individuals showing A− into four groups: CU (A−T−, n = 31), non-AD group (A−T−, n = 69), non-AD group (A−T+, n = 60), and PSP group (A−T+, n = 42) for plasma biomarker analysis. None of the participants had A+T− biomarker status in this study.

2.6 | Tau burden evaluation

We also classified the global tau loading for each subject into three levels of tau burden. The cutoffs for tau burden were derived from a data-driven and global brain VOI based on the methodology reported by Mattsson-Carlgren et al.[22] First, a data-driven VOI (AD-vulnerable VOI) was constructed by a voxel-wise comparison between two independent cohorts of CU A− and AD. Then a bi-Gaussian mixture model (GMM) was fitted on the histogram of SUVR within the AD-vulnerable VOI of a group of CU (A−), MCI (A+), and dementia (A+) subjects (Supplementary Methods). Subsequently, the participants were stratified into low, intermediate, and high tau deposition categories based on their SUVR values within the meta-VOI: low (SUVR < 1.45), intermediate (SUVR 1.45–2.12), and high (SUVR > 2.12), with cutoff values determined via the GMM analysis.

2.7 | Plasma biomarker measurements

The pre-analytical sample handling was consistent among hospitals (Supplementary Methods). AD core biomarkers (p-tau217, p-tau181, Aβ1-42, and Aβ1-40) and neurodegenerative biomarkers (NfL, GFAP) were analyzed using single-molecule array analysis. Plasma Aβ1-42 and Aβ1-40 levels were determined using a multiplex array (Neurology

3-Plex A Advantage Kit N3PA, Quanterix), and p-tau217, p-tau181, NfL, and GFAP levels were measured using other arrays (p-tau217, ALZpath V2, p-tau181 V2.1, Neurology 2-Plex B Kit Quanterix). Aβ42/40 represented the ratio between Aβ1-42 and Aβ1-40.

2.8 | Statistical analysis

The study analysis was based on two diagnostic categories. The first category was based on the clinical enrolment criteria, that is, CU, MCI, dementia, and PSP. The second category was based on the biological classification according to amyloid and tau PET, that is, CU (A−T−), AD (A+T+), non-AD (A−T+), non-AD (A−T−), and PSP (A−T+, 4R tau group). Continuous variables among these groups were analyzed using the *t* test or analysis of variance followed by Bonferroni correction as appropriate. Categorical data were analyzed using the chi-square test. Correlations were evaluated using Pearson correlation coefficients. Determining amyloid PET and tau PET positivity was conducted using receiver operating characteristic (ROC) curves, and comparisons of areas under the curve (AUCs) among established plasma biomarkers were performed using the DeLong test. Binary reference points for amyloid PET positivity and tau PET burden were derived based on the Youden index, and sensitivity, specificity, and positive and negative predictive agreements were thereby calculated. All statistical analyses were performed using R software version 4.2.1 (R Foundation for Statistical Computing). *p*-values < 0.05 were considered statistically significant.

3 | RESULTS

3.1 | Cohort demographics

There were 51 participants in the CU group, 104 in the MCI group, 163 in the dementia group, and 43 in the PSP group from the two independent Taiwan cohorts (Table 1, and Table S1). Amyloid (A±) and tau (T±) status was determined based on PET scans, and the amyloid-positive rates in the CU, MCI, dementia, and PSP groups were 10%, 34%, 61%, and 0%, respectively. There were significant group differences in all of the tested plasma biomarkers. In post hoc analysis, plasma p-tau181, p-tau217, and GFAP levels in the MCI and dementia groups were higher than those in the CU and PSP groups. In addition, there were significant differences in plasma Aβ42/40, p-tau181, p-tau217, and GFAP levels between the MCI (A+) and MCI (A−) or dementia (A+) and dementia (A−) groups (Table S2 in supporting information). Similar trends were noted between the CU (A+) and CU (A−) groups, but only p-tau181 and GFAP reached statistical significance.

3.2 | [18F]Florzolotau images of the five biological groups

Based on the amyloid and tau status (Figure 1A), the participants were classified into five biological status groups (Figure 1B): CU (A−T−), AD (A+T+), non-AD (A−T−), non-AD (A−T+), and PSP. Comparable tau patterns were found in the non-AD A−T− and CU A−T− group. In the non-AD (A−T+) groups, tau deposits were noted in the lateral temporal lobe and posterior region, while they were only noted in the subcortical region in the PSP group.

3.3 | Plasma biomarker comparisons among the biological groups

Comparisons among the p-tau217, p-tau181, GFAP, NfL, and Aβ42/40 plasma biomarkers among the five biological groups are shown in Figure 2. In the AD group, the plasma concentrations of p-tau217, p-tau181, and GFAP were significantly higher than those in the other four groups. In addition, the level of NfL in the PSP group was significantly higher than in the other three groups (CU, AD, and A−T−).

3.4 | Tau PET burden

Based on the AD-vulnerable VOIs and the SUVR histogram fitting (Figure S1 in supporting information), the patients with AD were stratified into three tau burden groups (see Figure 3A for the mean SUVR images). Compared to the low- and intermediate-tau burden groups, the high-tau burden group had higher mean tau loading in the neocortex (lateral temporal lobe, frontal lobe, parietal lobe, and occipital lobe; Figure 3B). There was a significantly increasing trend of SUVR in the Braak stage VOIs with increasing tau burden in the AD groups (Figure 3C). In addition, with increased tau burden, lower MMSE scores and higher CDR-SB scores were observed (Figure 3D).

3.5 | AUCs based on amyloid or tau status

To understand the discriminative ability of each plasma biomarker, we calculated the ROCs and reported the highest Youden index with related sensitivity and specificity. First, we compared the performance of the plasma biomarkers in predicting abnormal amyloid PET status with the maximum number of participants within each biomarker group (Figure 4A). Plasma p-tau217 (AUC: 0.946, confidence interval [CI]: 0.923–0.969) outperformed p-tau181 (AUC: 0.865, CI: 0.825–0.906), GFAP (AUC: 0.799, CI: 0.753–0.845), Aβ42/40 (AUC: 0.704, CI: 0.648–0.759), and NfL (AUC: 0.605, CI: 0.547–0.663) in identifying AD pathology (Figure 4A). In addition, the AUC of plasma p-tau217 did not significantly increase when adding demographics (age and education) and MMSE score into the prediction model (Table S3 in supporting information). Nonetheless, the highest discriminative ability was for amyloid Centiloid (AUC: 0.984, CI: 0.969–0.999).

Based on the research purposes, we then calculated the ROC to predict high versus low/intermediate tau burden, focusing on the participants who were amyloid PET–positive (Figure 4B). Plasma p-tau217 (AUC: 0.748, CI: 0.651–0.845) outperformed GFAP (AUC: 0.528, CI: 0.404–0.653) and NfL (AUC: 0.454, CI: 0.333–0.575), but was similar to p-tau181 (AUC: 0.713, CI: 0.606–0.820) and Aβ42/40 (AUC: 0.602,

TABLE 1 Demographic and biomarker data among clinical groups.

	CU ($n = 51$)	MCI ($n = 104$)	Dementia ($n = 163$)	PSP ($n = 43$)	*p*-value
Age, years[a]	65.3 (8.6, 57.8–71.3)	71.8 (7, 67.7–76.5)*	73.9 (7.6, 69.5–79.1)*,***	68.8 (7.6, 64.3–73.2)	<0.001
Education, years[a]	12.3 (4.2, 9–16)	10.2 (3.6, 6–12)*	8 (4.6, 6–12)*,**,***	11.3 (4.4, 6–15)	<0.001
MMSE[a]	28.2 (1.6, 27–29)	26.1 (1.9, 24.5–28)	17.3 (5.4, 14–22)*,**,***	22 (7.8, 21–27)*,**	<0.001
CDR[a]	0 (0, 0–0)	0.5 (0, 0.5–0.5)*	0.8 (0.5, 0.5–1)*,**,***	0.5 (0.6, 0–0.5)*	<0.001
CDR-SB[a]	0 (0, 0–0)	1.3 (1, 0.5–2)*	4.5 (3.1, 2.5–5.5)*,**,***	2.3 (3.9, 0–3.5)*	<0.001
Male, *n* (%)	23 (45)	56 (54)	61 (37)	20 (47)	0.07
APOE genotyping, *n* (%)					0.005
APOE ε4 carrier	13 (25)	23 (22)	66 (40)	10 (23)	
Missing data	2 (4)	1 (1)	4 (2)	2 (5)	
Amyloid PET positive, *n* (%)	5 (10)	35 (34)	99 (61)	0 (0)	<0.001
Receiving tau PET, *n* (%)	42 (82)	97 (93)	140 (86)	43 (100)	0.001
PET status, *n* (%)					<0.001
A(+)/T(+)	3 (6)	31 (30)	83 (51)	0 (0)	
A(+)/T(−)	0 (0)	1 (1)	0 (0)	0 (0)	
A(−)/T(+)	8 (16)	20 (19)	32 (19)	0 (0)	
A(−)/T(−)	31 (61)	45 (43)	24 (15)	0 (0)	
PSP	0 (0)	0 (0)	0 (0)	42 (98)	
A(+)/T(MD)	2 (4)	3 (3)	16 (10)	0 (0)	
A(−)/T(MD)	7 (13)	4 (4)	7 (4)	0 (0)	
A(−)/T(Motion)	0 (0)	0 (0)	1 (1)	1 (2)	
Plasma biomarkers[a]					
Aβ42/40	0.0511 (0.0146, 0.0402–0.0611)	0.0474 (0.0149, 0.0372–0.0579)***	0.0455 (0.0136, 0.0360–0.0543)***	0.057 (0.0155, 0.0438–0.0678)	<0.001
p-tau181, pg/mL	19.04 (6.44, 14.49–23.26)	28.03 (12.42, 20.21–32.93)*,***	34.32 (15.4, 22.37–44.23)*,**,***	20.04 (6.36, 14.94–23.32)	<0.001
p-tau217, pg/mL	0.262 (0.168, 0.171–0.333)	0.523 (0.395, 0.243–0.622)*,***	0.812 (0.52, 0.364–1.213)*,**,***	0.264 (0.123, 0.182–0.317)	<0.001
NfL, pg/mL	15.47 (12.77, 8.15–18.15)	25.4 (26.71, 13.65–24.65)*,***	29.7 (17.46, 17.43–36.14)*,***	41.46 (28.6, 21.38–53.16)*	<0.001
GFAP, pg/mL	183.8 (89.3, 115.2 –235.9)	293.6 (223, 137.9–417.8)*,***	401.2 (256.1, 221.7–527.3)*,**,***	185.1 (108.1, 100.4–247.6)	<0.001

Note: *APOE* genotype data were not available in 9 subjects, including 2 CU, 1 MCI, 4 dementia, and 2 PSP. PET visual score status was unavailable in 41 subjects due to (1) Tau PET not done in 9 CU, 7 MCI, 23 dementia subjects, and (2) motion artifact of Tau PET in 1 dementia and 1 PSP subjects.

Abbreviations: A(+)/A(−) amyloid PET visual score positive/negative; Aβ, amyloid beta; *APOE*, apolipoprotein E; CDR, Clinical Dementia Rating; CDR-SB, Clinical Dementia Rating Sum of Boxes; CU, cognitively unimpaired; GFAP, glial fibrillary acidic protein; MCI, mild cognitive impairment; MD, missing data; MMSE, Mini-Mental State Examination; NfL, neurofilament light chain; PET, positron emission tomography; PSP, progressive supranuclear palsy; T(+)/T(−) tau PET visual score positive/negative.

[a]Continuous data are expressed as mean (standard deviation, interquartile range).

*p-value < 0.05 compared to CU in Bonferroni post hoc analysis.

**p-value < 0.05 compared to MCI in Bonferroni post hoc analysis.

***p-value < 0.05 compared to PSP in Bonferroni post hoc analysis.

CI: 0.470–0.735). Moreover, the AUC of p-tau217 was markedly higher after adding demographics (age and education) and MMSE score into the prediction model (AUC: 0.850, CI: 0.760–0.940; Table S3).

3.6 | p-tau217 levels in AD tau burden prediction

To assess the effectiveness of p-tau217 in predicting AD tau burden, we first compared p-tau217 levels among the three tau burden groups (Figure 5A). The results showed that the low and intermediate tau groups did not significantly differ in p-tau217 levels but were both lower than the high tau group. We then combined the low and intermediate tau burden groups into a low/intermediate group. The results then showed that the levels of p-tau217 in the two AD tau groups were significantly higher than in the PSP or non-AD (A–T+) tau group (Figure 5B). Likewise, in the p-tau181 and GFAP levels, the two AD tau burden groups also exhibited statistically significantly higher values (Figure 5B). As shown in Figure 5C, voxel-wise correlation analysis showed the topographic covariation of p-tau217 with

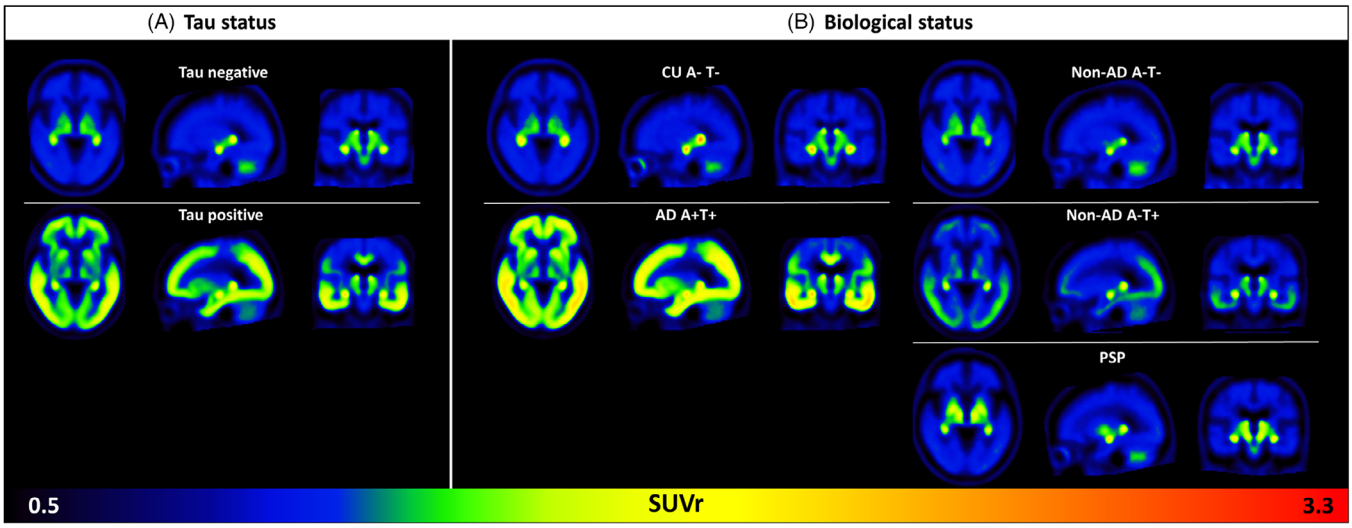

FIGURE 1 The mean tau PET images for (A) the tau-positive (T+) and negative (T−) groups based on the visual score (VS) assessment; (B) five biological groups: CU A−T−, AD A+T+, non-AD A−T−, non-AD A−T+, and PSP. All PET images are displayed in SUVR from 0.5 to 3.3. ** The five biological statuses are based on amyloid and tau positivity evaluated by visual reading. A−, amyloid negative; A+, amyloid positive; AD, Alzheimer's disease; CU, cognitively unimpaired; PET, positron emission tomography; PSP, progressive supranuclear palsy; SUVR, standardized uptake value ratio

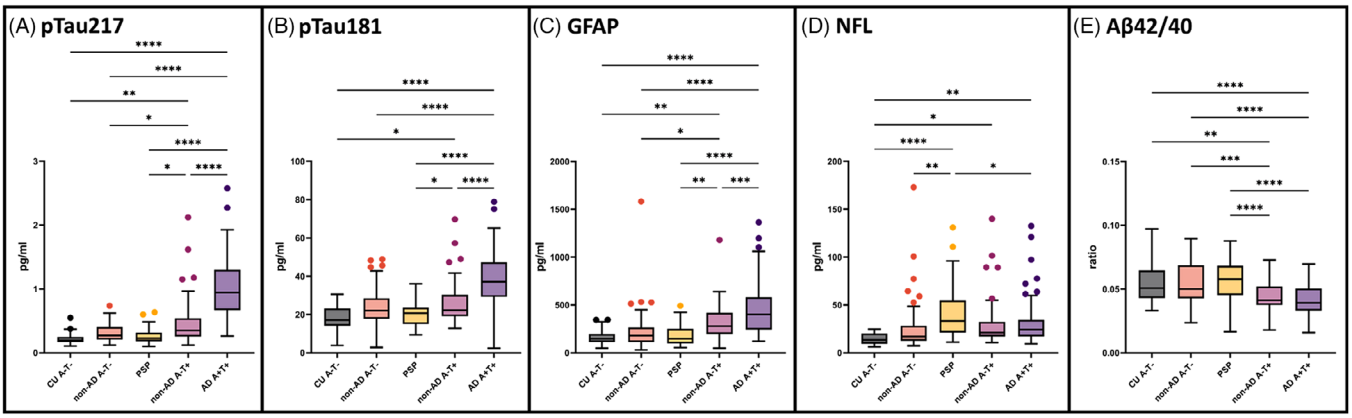

FIGURE 2 Box plots displaying plasma biomarker levels for (A) p-tau217, (B) p-tau181, (C) GFAP, (D) NfL, and (E) Aβ42/40 across the five biological groups with post hoc analysis. * $p < 0.05$, ** $p < 0.01$, *** $p < 0.005$, **** $p < 0.0001$. Box plots show the median, lower and upper quartiles, and outliers using dots. A−, amyloid negative; A+, amyloid positive; Aβ, amyloid beta; AD, Alzheimer's disease; CU, cognitively unimpaired; GFAP, glial fibrillary acidic protein; NfL, neurofilament light chain; PET, positron emission tomography; PSP, progressive supranuclear palsy; p-tau, phosphorylated tau; T+, tau positive; T−, tau negative

tau PET in the AD group. A significant correlation between p-tau217 level and clinical MMSE and CDR-SB scores was also observed (Figure 5D). Regions in tau PET showing positive correlations with p-tau181, Aβ42/40, GFAP, NfL in AD (Figure S2 in supporting information), PSP (Figure S3 in supporting information), A−T− non-AD (Figure S4 in supporting information), and A−T+ non-AD (Figure S5 in supporting information) groups and their relationships with cognitive measures are illustrated separately. The ROC analysis for predictive performance of each biomarker for amyloid positivity response (Figure S6 in supporting information) or for low/intermediate versus high tau burden in AD subjects (Figure S7 in supporting information) within two hospital cohorts were calculated.

3.7 | First step reference points for amyloid positivity

We first derived the binary reference points for amyloid PET positivity using the Youden index from the Kaohsiung cohort, and then cross-validated the results in the Linkou cohort (Table 2). The reference point of p-tau217 was estimated to be 0.562 pg/mL, with sensitivity and specificity > 0.85 in both cohorts. In the MCI subgroup using this cutoff value (Table 2), the specificity and sensitivity were 0.942 and 0.8, respectively, with an overall percent agreement (OPA) of 0.894. There were 60 patients with early-stage dementia in this study (Supplementary Methods, Table S4 in supporting information). In the

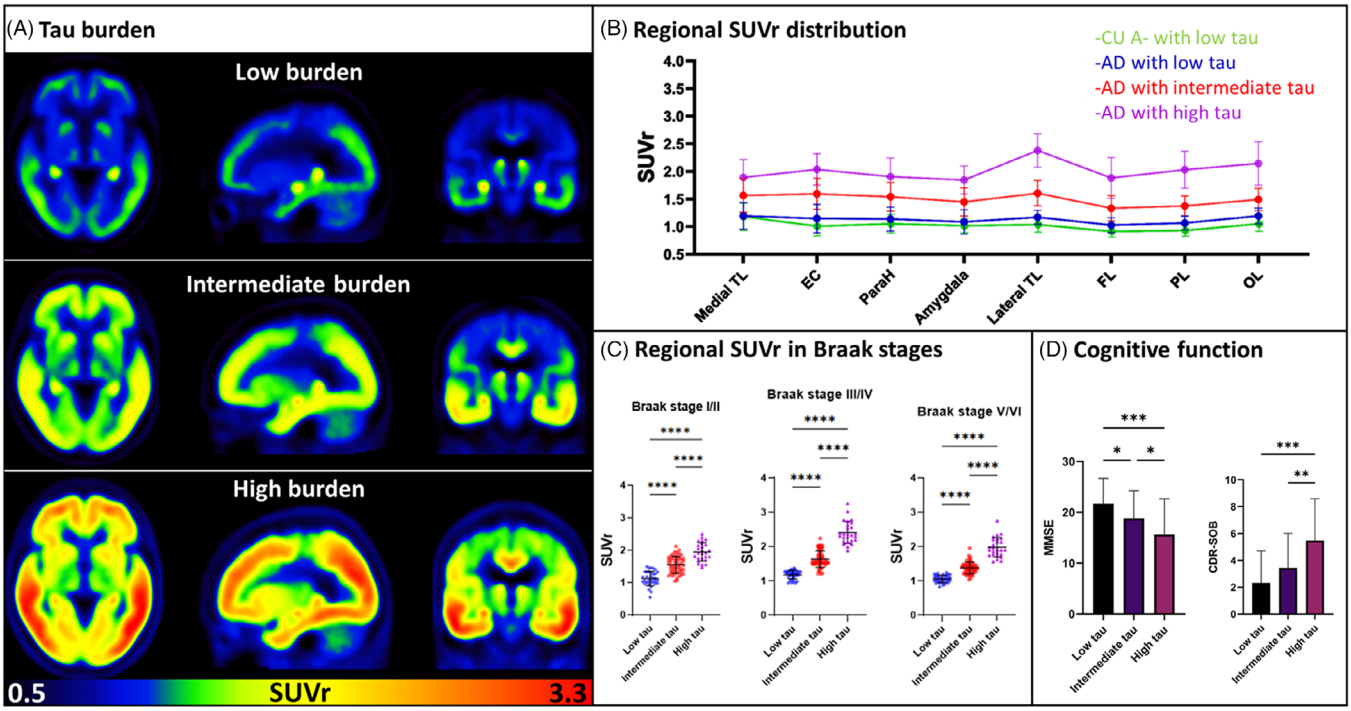

FIGURE 3 A, Average tau PET images by low, intermediate, or high tau burden groups. B, Regional SUVR distribution in CU (A−T−) and AD (A+T+) groups, stratified by three tau burden groups. C, Comparisons of regional SUVR in Braak stage VOIs. D, cognitive functions of MMSE and CDR-SB among three tau burden groups in AD (A+T+). PET images are displayed in SUVR ranging from 0.5 to 3.3. All of the statistical graphs are plotted as mean with standard deviation. All of the statistical graphs are plotted as mean values with standard deviation. * $p < 0.05$, ** $p < 0.01$, *** $p < 0.005$, **** $p < 0.0001$. A−, amyloid negative; A+, amyloid positive; AD, Alzheimer's disease; CDR-SB, Clinical Dementia Rating Sum of Boxes; CU, cognitively unimpaired; EC, entorhinal cortex; FL, frontal lobe; MMSE, Mini-Mental State Examination; OL, occipital lobe; ParaH, parahippocampus; PET, positron emission tomography; PL, parietal lobe; SUVR, standardized uptake value ratio; T+, tau positive; T−, tau negative; TL, temporal lobe; VOIs, volumes of interest

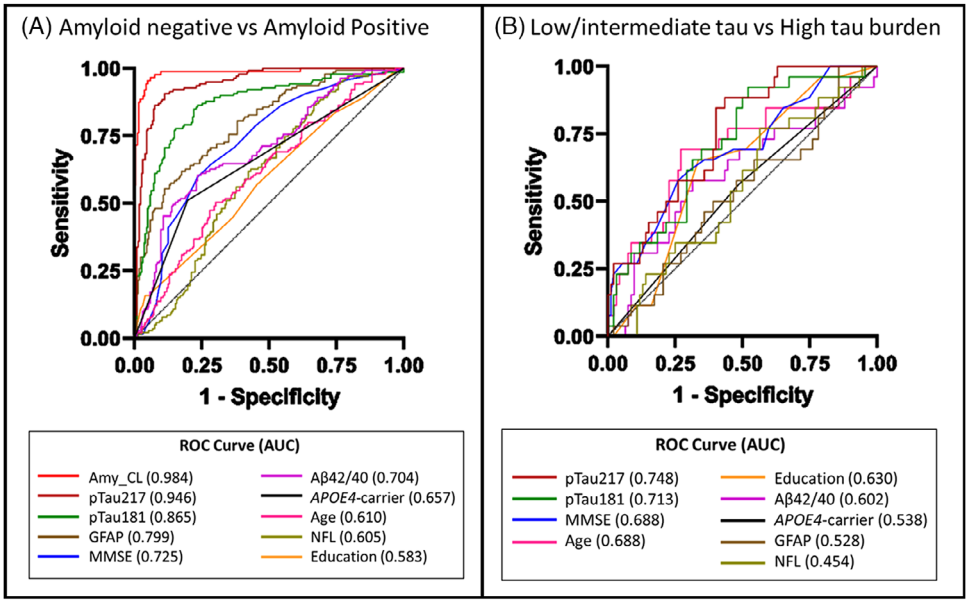

FIGURE 4 Receiver operating characteristic (ROC) curve analyses for amyloid PET positivity in all participants (A), and tau burden in amyloid PET−positive participants (B). Aβ, amyloid beta; Amy_CL, amyloid Centiloid; *APOE*, apolipoprotein E; AUC, area under the curve; GFAP, glial fibrillary acidic protein; MMSE, Mini-Mental State Examination; NfL, neurofilament light chain; PET, positron emission tomography; p-tau, phosphorylated tau

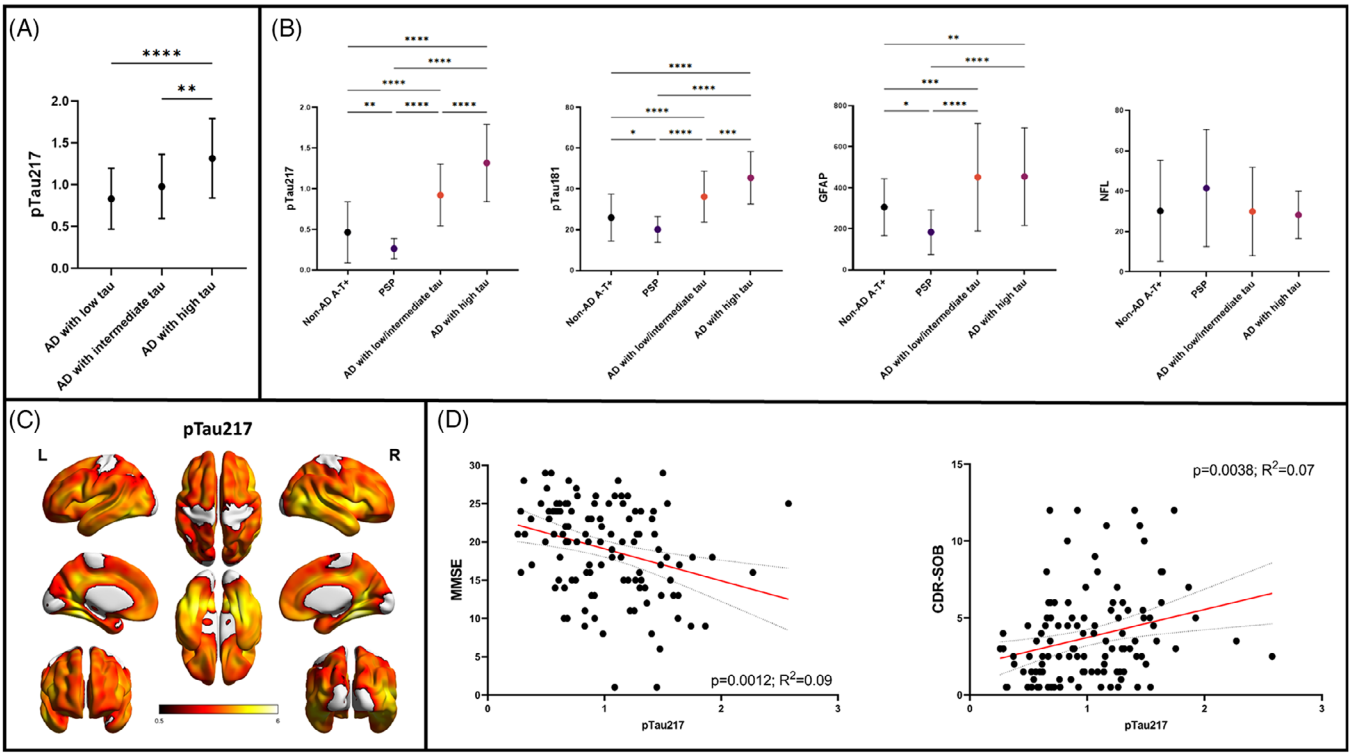

FIGURE 5 A, Comparison of p-tau217 levels (mean with standard deviation) among the three different tau burden groups (low, intermediate, and high) in AD. B, Comparisons of p-tau217, p-tau181, GFAP, and NfL levels (left to right) among the individuals with non-AD A−T+ tauopathy, PSP, AD with low/intermediate tau burden, and AD with high tau burden. C, Topographic representation illustrating the covariation of p-tau217 with tau PET in the AD group, adjusted for age and sex with $p < 0.01$, cluster size 100 voxels, and $t[0.5–6]$ for visualization. D, Regression lines with 95% confidence intervals depicting the relationship between p-tau217 and MMSE or CDR-SB. All of the statistical graphs are plotted as mean values with standard deviation. * $p < 0.05$, ** $p < 0.01$, *** $p < 0.005$, **** $p < 0.0001$. AD, Alzheimer's disease; CDR-SB, Clinical Dementia Rating Sum of Boxes; GFAP, glial fibrillary acidic protein; MMSE, Mini-Mental State Examination; NfL, neurofilament light chain; PET, positron emission tomography; PSP, progressive supranuclear palsy; p-tau, phosphorylated tau

early AD group using the p-tau217 cutoff level of 0.562 pg/mL, the specificity, sensitivity, and accuracy were 0.941, 0.925, and 0.934, respectively, with positive predictive agreement (PPA), negative predictive agreement (NPA), and OPA values of 0.942, 0.925, and 0.935, respectively. When applied in the patients with cognitive deficits (combining MCI and dementia groups), plasma p-tau217 could accurately identify A+ cases, with sensitivity and specificity > 0.85; however, the sensitivity dropped to 0.60 in the CU group. The reference points of p-tau181 (29.2 pg/mL), GFAP (360.7 pg/mL), NfL (20.94 pg/mL), and Aβ42/40 ratio (0.039) were also derived for abnormal amyloid PET, but with less consistency compared to p-tau217 (Table S5 in supporting information).

3.8 | Second step reference points using p-tau217 to predict tau PET burden

We next derived the reference points of plasma p-tau217 based on the Kaohsiung cohort to differentiate amyloid PET-positive patients with low/intermediate tau PET burden from those with high tau PET burden (Table 2). The reference point of p-tau217 was estimated to be 0.964 pg/mL, with relatively high specificity and PPA to identify low/intermediate tau burden in both cohorts and in each diagnostic group (Table 2). P-tau181 had similar trends to p-tau217, but the discriminative ability of the other biomarkers was relatively inconsistent (Table S6 in supporting information).

4 | DISCUSSION

Based on cohorts from two independent memory clinics in the T-ADNI, we propose a two-step workflow (Figure 6) toward integrating plasma p-tau217 for potential patients showing A+ PET and low-to-intermediate tau burden. The ultimate goal for this workflow was to find candidates suitable for AD anti-amyloid therapy who may show a favorable response.[2,3,37–39] In the first step, our findings demonstrated that p-tau217 reached the highest accuracy (AUC = 0.94) in identifying amyloid PET positivity among five commercially available plasma biomarkers. When applying the p-tau217 results to the patients with cognitive deficits ($n = 267$), a binary approach demonstrated high sensitivity, specificity, and positive and negative predictive agreements (all > 0.87) for p-tau217. Even though there were only 51 participants in the CU group, the high specificity and positive and negative predictive agreements indicate a possible screening strategy for preclinical cases.

TABLE 2 Binary references of plasma p-tau217 for amyloid positivity and low/intermediate tau burden.

Binary reference for amyloid PET positivity: plasma p-tau217 > 0.562 pg/mL							
	Sites			Clinical diagnosis			
	KHS	LK	All	CU	MCI	Dementia	PCD
Case no.	254	107	361	51	104	163	267
Amyloid PET positive, *n* (%)	119	20	139 (39)	5	35	99	134
Plasma p-tau217 status positive, *n* (%)	113	24	137 (38)	3	32	100	132
Sensitivity	0.866	0.850	0.863	0.600	0.800	0.899	0.873
Specificity	0.926	0.920	0.923	1.000	0.942	0.828	0.887
PPA	0.912	0.708	0.876	1.000	0.875	0.890	0.886
NPA	0.887	0.964	0.915	0.958	0.903	0.841	0.874
OPA	0.898	0.907	0.900	0.961	0.894	0.871	0.880
Binary reference for low/intermediate tau burden in amyloid PET positive cases: plasma p-tau217 < 0.964 pg/mL							
	Sites			Clinical diagnosis			
	KHS	LK	All	CU	MCI	Dementia	
Case no.	101	17	118	3	32	83	
Low/intermediate Tau PET burden, *n*	90	12	92	3	29	60	
Plasma p-tau217 status positive, *n*	50	9	59	2	21	36	
Sensitivity	0.588	0.667	0.598	0.667	0.690	0.550	
Specificity	0.857	0.800	0.846	–	0.667	0.870	
PPA	0.940	0.889	0.932	1.000	0.952	0.917	
NPA	0.353	0.500	0.373	0.000	0.182	0.426	
OPA	0.644	0.706	0.653	0.667	0.688	0.639	

Note: Tau burden based on [18F]Florzolotau PET.
Abbreviations: CU, cognitively unimpaired; LK, Linkou Chang Gung Memorial Hospital; KHS, Kaohsiung Chang Gung Memorial Hospital; MCI, mild cognitive impairment; NPA, negative predictive agreement; OPA, overall agreement; PCD, patients with cognitive deficits; PET, positron emission tomography; PPA, positive predictive agreement; p-tau, phosphorylated tau.

From a cost-effective point of view, using the identified cutoff value of p-tau217 could have saved 94% of the confirmative amyloid PET scans in the CU group, 69.2% in the MCI group, and 38.7% in the dementia group. In total, 57.5% of the amyloid PET could have been saved by using the p-tau217 cutoff value.

As amyloid Centiloid still showed the highest AUC among p-tau217 alone, p-tau217 and demographics, and p-tau217 with MMSE score and demographics, our results support the notion that a confirmative amyloid PET is mandatory for establishing a diagnosis of AD, especially in those intending to participate in anti-amyloid therapy. At present, amyloid PET should not be replaced by plasma biomarkers, whether used alone or in combination with other data. Based on the individuals with positive amyloid PET results, we further calculated a second binary p-tau217 cutoff value. The high positive predictive agreements of p-tau217 indicated its potential in identifying cases showing low/intermediate tau burden as derived from [18F]Florzolotau PET.

Previous studies have shown that of current diagnostic and prognostic tools related to amyloid and tau pathology, p-tau217 plasma biomarkers yield the best results,[40,41] and that they are well correlated with cerebrospinal fluid levels[40] and can differentiate other neurodegenerative disorders.[42] To understand the properties of p-tau217 on tauopathies, we included two A−T+ groups and compared them to AD patients showing A+T+. One of the A−T+ groups could possibly have represented primary age-related tauopathy (PART).[43] PART is a pathological term but with overlapping clinical phenotypes[44,45] and tau isoforms with AD in cryo-electron microscopy.[11] As a clinical consensus regarding PART is not currently available, the combination of amyloid and tau PET has allowed for the *ante mortem* diagnosis of PART.[46] Our AD patients had significantly higher p-tau217 levels compared to those with PART, supporting the specificity of p-tau217 to elucidate the underlying amyloid pathology. The feasibility of p-tau217 to discriminate between PET-confirmed PART and AD is particularly important from a treatment perspective, as anti-amyloid therapies may only be effective in patients with AD. P-tau217 can also be considered a biomarker for mixed-type (i.e., 3R+4R) tauopathy based on our significant voxel-wise correlations using [18F]Florzolotau PET and the significant correlations with cognitive measures in AD and PET-confirmed PART. This forms a rationale for our proposal of using p-tau217 cutoff levels to reflect a binary tau burden in amyloid-positive cases.

PSP represents tauopathy mainly with 4R tau,[47] while high in vivo specificity has been shown in the basal ganglia and midbrain

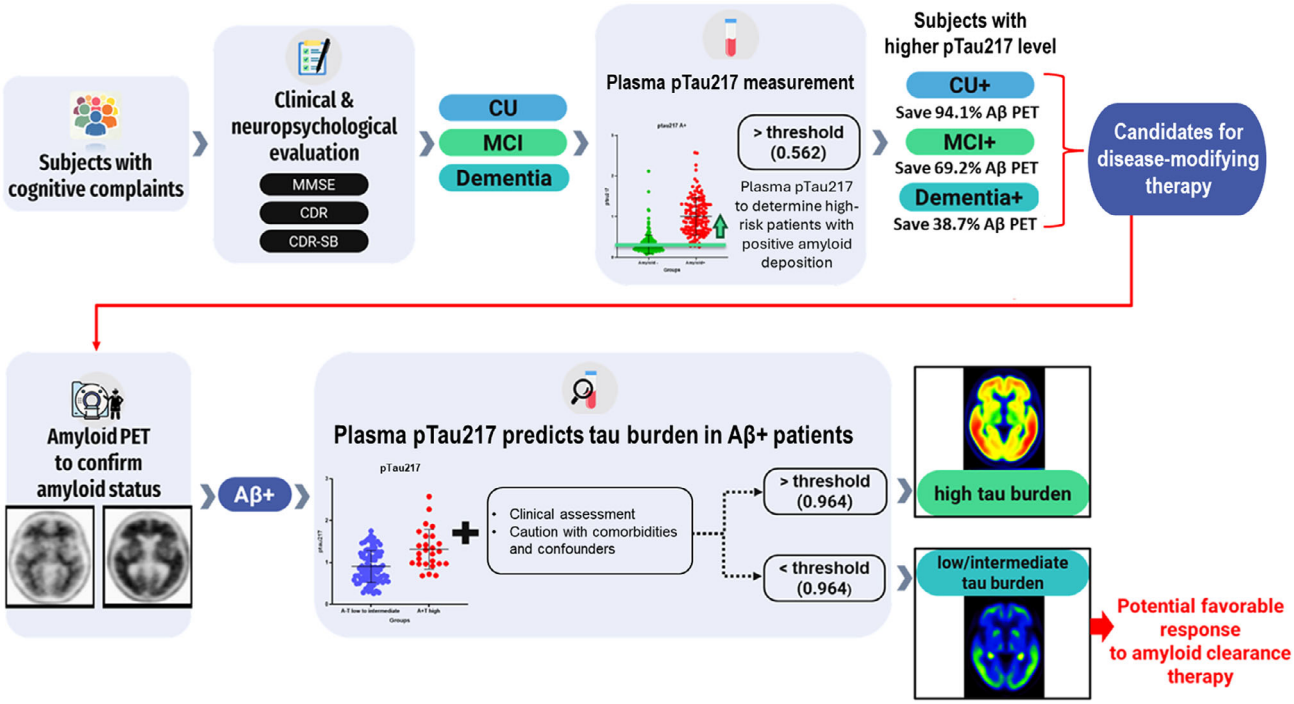

FIGURE 6 A potential two-step workflow to integrate p-tau217 to identify amyloid PET–positive cases and predict tau burden. Thresholds listed are based on the Taiwan ADNI cohorts. Aβ, amyloid beta; AD, Alzheimer's disease; ADNI, Alzheimer's Disease Neuroimaging Initiative; CU, cognitively unimpaired; CDR, Clinical Dementia Rating; CDR-SB, Clinical Dementia Rating Sum of Boxes; MMSE, Mini-Mental State Examination; MCI, mild cognitive impairment; PET, positron emission tomography; p-tau, phosphorylated tau

regions using [18F]Florzolotau PET.[13,48] NfL is considered a non-specific biomarker, and higher levels of NfL have been reported in patients with PSP and others.[49–53] In our analysis, we found that a significantly high NfL level and p-tau217 level within normal range could enhance the clinical diagnostic accuracy of PSP, as the patterns were different from the AD, PET-confirmed PART, and non-AD groups. In addition, NfL levels were also significantly correlated with cognitive performance in the patients with PSP. On the other hand, a direct comparison of biomarkers between the PSP and PET-confirmed PART groups enabled comparing the role of plasma biomarkers in 4R versus mixed-type tauopathies without confounding amyloid. The patients with PART had significantly higher levels of p-tau217 compared to those with PSP. The significant correlation between p-tau217 and [18F]Florzolotau SUVR signals or between p-tau217 and cognitive measures in the PET-confirmed PART group suggests that p-tau217 shows more specificity for mixed type (3R+4R) tauopathy.

To assess tau burden in the amyloid-positive population for guiding decisions regarding anti-amyloid treatment, we used a bi-Gaussian mixture model to analyze SUVRs within the AD-vulnerable VOI, determining thresholds indicative of tau levels. Existing literature offers varied methodologies for establishing tau cutoffs across different VOIs. Notably, cutoffs derived from global VOIs exhibit superior efficacy in staging and classification compared to those from regional tau VOIs, such as medial temporal VOI or the inferior temporal lobe. Conversely, regional cutoffs may demonstrate higher sensitivity in early detection and memory decline.[54] Recent investigations have observed the diversity of tau distribution patterns among AD patients. Cutoffs derived exclusively from the temporal region may inadequately capture tau burden, particularly in atypical AD cases featuring a temporal-sparing tau pattern.[55] Consequently, researchers have explored data-driven or multiple anatomical-region approaches, incorporating AD-vulnerable regions, Braak stage VOIs, and combinations of the medial temporal lobe and neocortex.[22,55,56] Our study adopts the AD-vulnerable VOI, a data-driven method encompassing regions demonstrating significant differences between CU individuals and amyloid-positive AD patients. This global VOI effectively reflects tau loading in the human brain and demonstrates robust performance in distinguishing between high and low/intermediate tau burdens.

Both visual assessment and quantitative cutoffs are common practices in nuclear medicine imaging to determine the positivity of PET, each with its own pros and cons. Although the amyloid PET ligands used in this study have received regulatory approval for clinical use, results by visual assessment can still be influenced by the raters' experience, which resulted in inter-rater variability.[17] On the other hand, using quantitative methods to determine tau cutoffs is comparatively more objective but the variabilities can be related to the processing steps, VOIs, or the reference group used.[19] Although the semiquantitative cutoff values for amyloid and tau PET images demonstrated equivalent diagnostic accuracy compared to visual reading here, the inconsistency also highlighted the importance of integrating complementary information by these two methods.[20] Future work exploring the hybrid approach to leverage the strengths of both methodologies is needed.

We included plasma levels of GFAP in our analysis to reflect reactive astrogliosis after amyloid and tau pathologies.[57,58] Evidence has indicated that astrogliosis contributes to the pathogenesis of AD at different pathological stages[8,59,60] or co-pathologies.[61] In our analysis, we found a significantly higher level of GFAP in the AD group compared to the other four diagnostic groups. Paradoxically, we did not establish the predictive role of GFAP for cognitive measures or tau burden (Figure 5 between low–intermediate vs. high tau burden) in the AD group. Therefore, our results only support that plasma GFAP may reflect the presence of amyloid in AD, but that it is not related to tau burden or cognitive status in AD. The finding that plasma GFAP may be an early marker associated with amyloid pathology but not tau aggregation is similar to a previous report.[60] In contrast, cerebrospinal fluid YKL-40 may be a more specific biomarker for reflecting amyloid and tau based on its mediation role in AD.[7]

Our analysis has several limitations. First, the role of p-tau217 in predicting amyloid positivity in CU individuals was established in the BioFINDER,[62] AIBL,[63] and WRAP[41] cohorts; however, we found a lower sensitivity of p-tau217 when using our cutoff value in the CU group (0.6) compared to the patients with cognitive deficits (0.87). This finding may reflect that p-tau217 is of less practical utility in discriminating A+/A− status in CU individuals. A prospective study enrolling more CU cases may help to elucidate the problems related to the small number of cases and may lead to revisions in the cutoff value. Second, among the preselected biomarkers, p-tau217 emerged as the most important tool for AD screening, as it is more accessible and can differentiate cases with AD brain pathology from others. The binary levels of our proposed p-tau217 cutoffs had lower sensitivity and higher specificity in the MCI patients, and higher sensitivity and lower specificity in the patients with dementia. Therefore, the direct application of one p-tau217 reference level to all patients with cognitive deficits may not be fully appropriate. Cognitive severity-based cutoff values in patients with MCI or dementia may optimize its screening ability. Third, a subset of patients may develop AD before 65 years of age, termed EOAD. In general, EOAD comprises ≈ 5% of AD patients and it differs substantially from late-onset AD in the clinical, neuropsychological, neuroimaging, genetic, and neuropathological aspects.[64] In this study, the percentage of MCI and dementia patients with onset age < 65 years was 10.6% and 11%, respectively. In this context, plasma p-tau217 still had the highest AUC among the tested plasma biomarkers to differentiate amyloid PET positivity when applied to participants with EOAD (AUC: 0.979, CI: 0.947–1.000) and late-onset AD (AUC: 0.937, CI: 0.909–0.964; data not shown). As the analysis was based on small case numbers, future studies with larger sample size and longitudinal follow-up are warranted to delineate the clinical utility of p-tau217 for diagnosis or staging in patients with EOAD.[65] Finally, favorable outcomes after anti-amyloid therapy involve multiple factors including age and *APOE* ε4 status, and do not solely depend on tau burden. The cutoff level of p-tau217 to reflect tau burden reported in this study was based on [18F]Florzolotau PET analysis. Further studies are needed to confirm whether this cutoff value could also be applied to other tau tracers.

In summary, we found that integrating p-tau217 into the screening strategy for AD could help reduce the number of unnecessary amyloid PET scans. For amyloid PET–positive individuals, the high positive predictive agreement of p-tau217 could improve the prediction of tau burden, which may enhance treatment outcomes and shared decision making regarding disease-modifying therapies. The use of NfL, p-tau217, and [18F]Florzolotau can increase the diagnostic accuracy of PSP and prediction of cognition.

ACKNOWLEDGMENTS

The authors thank the patients and families for their participation in the study. This research was supported by Chang Gung Memorial Hospital, Taiwan (grant numbers CORPG8N0041, CMRPG8J0524, CMRPG8J0843, CMRPG3P0861, CMRPD1N0401, BMRP-488, and CMRPG8K1533) and the National Science and Technology Council, Taiwan (grant number NSTC 112-2321-B-182A-004, NSTC 112-2314-B-182-053, NSTC 113-2314-B-182-042-MY2, NSTC 113-2321-B-182A-005, and NSTC 110-2314-B-182A-073-MY3). We would like to thank Dr. Tzu-Chen Yen from Novascope Diagnostics Inc. and Dr. Ming-Kuei Jang from Aprinoia Therapeutics for the supports. We would like to acknowledge the administrative assistance from the clinical trial center of Linkou Chang Gung Memorial Hospital (CPRPG3H0011, PMRPG3K0011~PMRPG3K0014 and MOHW109-TDU-B-212-114005).

CONFLICT OF INTEREST STATEMENT

The authors have no conflicts of interest to declare that are relevant to the content of this article. Author disclosures are available in the supporting information.

CONSENT STATEMENT

We confirmed that all human subjects provided informed consent for this study.

ORCID

Kuo-Lun Huang https://orcid.org/0000-0001-8215-721X
Chiung-Chih Chang https://orcid.org/0000-0002-6721-2556

REFERENCES

1. Jack CR Jr, Bennett DA, Blennow K, et al. NIA-AA Research Framework: toward a biological definition of Alzheimer's disease. *Alzheimers Dement*. 2018;14:535-562.
2. Sims JR, Zimmer JA, Evans CD, et al. Donanemab in early symp-tomatic Alzheimer disease: the TRAILBLAZER-ALZ 2 randomized clinical trial. *JAMA*. 2023;330:512-527.
3. Pontecorvo MJ, Lu M, Burnham SC, et al. Association of donanemab treatment with exploratory plasma biomarkers in early symp-tomatic Alzheimer disease: a secondary analysis of the TRAILBLAZER-ALZ randomized clinical trial. *JAMA Neurol*. 2022;79:1250-1259.
4. Keshavan A, Pannee J, Karikari TK, et al. Population-based blood screening for preclinical Alzheimer's disease in a British birth cohort at age 70. *Brain*. 2021;144:434-449.
5. Langford O, Raman R, Sperling RA, et al. Predicting amyloid burden to accelerate recruitment of secondary prevention clinical trials. *J Prev Alzheimers Dis*. 2020;7:213-218.

6. Brum WS, Cullen NC, Janelidze S, et al. A two-step workflow based on plasma p-tau217 to screen for amyloid beta positivity with further confirmatory testing only in uncertain cases. *Nat Aging*. 2023;3:1079-1090.
7. Pelkmans W, Shekari M, Brugulat-Serrat A, et al. Astrocyte biomarkers GFAP and YKL-40 mediate early Alzheimer's disease progression. *Alzheimers Dement*. 2024;20:483-493.
8. Chatterjee P, Pedrini S, Doecke JD, et al. Plasma Abeta42/40 ratio, p-tau181, GFAP, and NfL across the Alzheimer's disease continuum: a cross-sectional and longitudinal study in the AIBL cohort. *Alzheimers Dement*. 2023;19:1117-1134.
9. Dittrich A, Ashton NJ, Zetterberg H, et al. Plasma and CSF NfL are differentially associated with biomarker evidence of neurodegeneration in a community-based sample of 70-year-olds. *Alzheimers Dement (Amst)*. 2022;14:e12295.
10. Li L, Liu FT, Li M, et al. Clinical utility of (18) F-APN-1607 tau PET imaging in patients with Progressive Supranuclear Palsy. *Mov Disord*. 2021;36:2314-2323.
11. Tagai K, Ono M, Kubota M, et al. High-contrast in vivo imaging of tau pathologies in Alzheimer's and non-Alzheimer's disease tauopathies. *Neuron*. 2021;109:42-58. e48.
12. Li J, Kumar A, Langstrom B, Nordberg A, Agren H. Insight into the binding of first- and second-generation PET tracers to 4R and 3R/4R tau protofibrils. *ACS Chem Neurosci*. 2023;14:3528-3539.
13. Li XY, Jiao FY, Yao RX, et al. The monoamine oxidase-B inhibitor selegiline does not affect (18) F-florzolotau up-take in patients with Progressive Supranuclear Palsy: a longitudinal case series. *Mov Disord*. 2023;38:705-707.
14. Endo H, Tagai K, Ono M, et al. A machine learning-based approach to discrimination of tauopathies using [(18) F]PM-PBB3 PET images. *Mov Disord*. 2022;37:2236-2246.
15. Shi Y, Murzin AG, Falcon B, et al. Cryo-EM structures of tau filaments from Alzheimer's disease with PET ligand APN-1607. *Acta Neuropathol*. 2021;141:697-708.
16. Jack CR Jr, Andrews JS, Beach TG, et al. Revised criteria for diagnosis and staging of Alzheimer's disease: Alzheimer's Association Workgroup. *Alzheimers Dement*. 2024;20:5143-5169.
17. Amadoru S, Dore V, McLean CA, et al. Comparison of amyloid PET measured in Centiloid units with neuropathological findings in Alzheimer's disease. *Alzheimers Res Ther*. 2020;12:22.
18. Matsuda H, Okita K, Motoi Y, et al. Clinical impact of amyloid PET using (18)F-florbetapir in patients with cognitive impairment and suspected Alzheimer's disease: a multicenter study. *Ann Nucl Med*. 2022;36:1039-1049.
19. Weigand AJ, Maass A, Eglit GL, Bondi MW. What's the cut-point?: a systematic investigation of tau PET thresholding methods. *Alzheimers Res Ther*. 2022;14:49.
20. Jack CR Jr, Wiste HJ, Weigand SD, et al. Defining imaging biomarker cut points for brain aging and Alzheimer's disease. *Alzheimers Dement*. 2017;13:205-216.
21. Scholl M, Lockhart SN, Schonhaut DR, et al. PET imaging of tau deposition in the aging human brain. *Neuron*. 2016;89:971-982.
22. Mattsson-Carlgren N, Collij LE, Stomrud E, et al. Plasma biomarker strategy for selecting patients with Alzheimer disease for antiamyloid immunotherapies. *JAMA Neurol*. 2024;81:69-78.
23. Landau SM, Lee J, Murphy A, et al. Individuals with Alzheimer's disease and low tau burden: characteristics and implications. *Alzheimers Dement*. 2024;20:2113-2127.
24. Johnson K, Li D, Dhadda S, et al. Biomarker assessments from clarity AD: downstream implications of targeting protofibrils and tau as a predictive biomarker. Clinical Trials on Alzheimer's Disease Conference. Boston, MA. 2023.
25. Langbaum JB, Zissimopoulos J, Au R, et al. Recommendations to address key recruitment challenges of Alzheimer's disease clinical trials. *Alzheimers Dement*. 2023;19:696-707.
26. Weber CJ, Carrillo MC, Jagust W, et al. The Worldwide Alzheimer's Disease Neuroimaging Initiative: ADNI-3 updates and global perspectives. *Alzheimers Dement (N Y)*. 2021;7:e12226.
27. Chang HI, Chang YT, Huang CW, et al. Structural covariance network as an endophenotype in Alzheimer's disease-suscep-tible single-nucleotide polymorphisms and the correlations with cognitive outcomes. *Front Aging Neurosci*. 2021;13:721217.
28. Hoglinger GU, Respondek G, Stamelou M, et al. Clinical diagnosis of progressive supranuclear palsy: the movement disorder society criteria. *Mov Disord*. 2017;32:853-864.
29. Ruwanpathirana GP, Williams RC, Masters CL, Rowe CC, Johnston LA, Davey CE. Inter-scanner Abeta-PET harmonization using barrel phantom spatial resolution matching. *Alzheimers Dement (Amst)*. 2024;16:e12561.
30. Ikari Y, Akamatsu G, Nishio T, et al. Phantom criteria for qualification of brain FDG and amyloid PET across different cameras. *EJNMMI Phys*. 2016;3:23.
31. Joshi A, Koeppe RA, Fessler JA. Reducing between scanner differences in multi-center PET studies. *Neuroimage*. 2009;46:154-159.
32. Lin HC, Lin KJ, Huang KL, et al. Visual reading for [(18)F]Florzolotau ([(18)F]APN-1607) tau PET imaging in clinical assessment of Alzheimer's disease. *Front Neurosci*. 2023;17:1148054.
33. Yang L, Rieves D, Ganley C. Brain amyloid imaging–FDA approval of florbetapir F18 injection. *N Engl J Med*. 2012;367:885-887.
34. Seibyl J, Catafau AM, Barthel H, et al. Impact of training method on the robustness of the visual assessment of 18F-Florbetaben PET scans: results from a Phase-3 study. *J Nucl Med*. 2016;57:900-906.
35. Jack CR Jr, Bennett DA, Blennow K, et al. NIA-AA research framework: toward a biological definition of Alzheimer's disease. *Alzheimers Dement*. 2018;14:535-562.
36. Dubois B, Villain N, Frisoni GB, et al. Clinical diagnosis of Alzheimer's disease: recommendations of the International Working Group. *Lancet Neurol*. 2021;20:484-496.
37. Hayato S, Takenaka O, Sreerama Reddy SH, et al. Population pharmacokinetic-pharmacodynamic analyses of amyloid positron emission tomography and plasma biomarkers for lecanemab in subjects with early Alzheimer's disease. *CP-T Pharmacometrics Syst Pharmacol*. 2022;11:1578-1591.
38. McDade E, Cummings JL, Dhadda S, et al. Lecanemab in patients with early Alzheimer's disease: detailed results on biomarker, cognitive, and clinical effects from the randomized and open-label extension of the phase 2 proof-of-concep-t study. *Alzheimers Res Ther*. 2022;14:191.
39. Gueorguieva I, Willis BA, Chua L, et al. Donanemab exposure and efficacy relationship using modeling in Alzheimer's disease. *Alzheimers Dement (N Y)*. 2023;9:e12404.
40. Ashton NJ, Brum WS, Di Molfetta G, et al. Diagnostic accuracy of a plasma phosphorylated tau 217 immunoassay for Alzheimer disease pathology. *JAMA Neurol*. 2024;81:255-263.
41. Jonaitis EM, Janelidze S, Cody KA, et al. Plasma phosphorylated tau 217 in preclinical Alzheimer's disease. *Brain Commun*. 2023;5:fcad057.
42. Palmqvist S, Janelidze S, Quiroz YT, et al. Discriminative accuracy of plasma phospho-tau217 for Alzheimer disease vs other neurodegenerative disorders. *JAMA*. 2020;324:772-781.
43. Crary JF, Trojanowski JQ, Schneider JA, et al. Primary age-related tauopathy (PART): a common pathology associated with human aging. *Acta Neuropathol*. 2014;128:755-766.
44. Duyckaerts C, Braak H, Brion JP, et al. PART is part of Alzheimer disease. *Acta Neuropathol*. 2015;129:749-756.
45. Elobeid A, Libard S, Leino M, Popova SN, Alafuzoff I. Altered proteins in the aging brain. *J Neuropathol Exp Neurol*. 2016;75:316-325.
46. Wuestefeld A, Pichet Binette A, Berron D, et al. Age-related and amyloid-beta-independent tau deposition and its downstream effects. *Brain*. 2023;146:3192-3205.

47. Martinez-Valbuena I, Lee S, Santamaria E, et al. 4R-Tau seeding activity unravels molecular subtypes in patients with Progressive Supranuclear Palsy. bioRxiv. 2023;2023.09.25.559953. doi:10.1101/2023.09.28.559953
48. Hong J, Lu J, Liu F, et al. Uncovering distinct progression patterns of tau deposition in Progressive Supranuclear Palsy using [(18)F]Florzolotau PET imaging and subtype/stage inference algorithm. *EBioMedicine*. 2023;97:104835.
49. Huang SY, Chen SF, Cui M, et al. Plasma biomarkers and positron emission tomography tau pathology in Progressive Supranuclear Palsy. *Mov Disord*. 2023;38:676-682.
50. Oliveira Hauer K, Pawlik D, Leuzy A, et al. Performance of [(18)F]RO948 PET, MRI and CSF neurofilament light in the differential diagnosis of Progressive Supranuclear Palsy. *Parkinsonism Relat Disord*. 2023;106:105226.
51. Bendstrup N, Hejl AM, Salvesen L. Neurofilament light chain levels in frontotemporal dementia and Progressive Supranuclear Palsy: a systematic review. *J Alzheimers Dis*. 2022;87:131-140.
52. Donker Kaat L, Meeter LH, Chiu WZ, et al. Serum neurofilament light chain in Progressive Supranuclear Palsy. *Parkinsonism Relat Disord*. 2018;56:98-101.
53. Rojas JC, Karydas A, Bang J, et al. Plasma neurofilament light chain predicts progression in Progressive Supranuclear Palsy. *Ann Clin Transl Neurol*. 2016;3:216-225.
54. Maass A, Landau S, Baker SL, et al. Comparison of multiple tau-PET measures as biomarkers in aging and Alzheimer's disease. *Neuroimage*. 2017;157:448-463.
55. Gogola A, Lopresti BJ, Tudorascu D, et al. Biostatistical estimation of tau threshold hallmarks (BETTH) algorithm for human tau PET imaging studies. *J Nucl Med*. 2023;64:1798-1805.
56. Chen SD, Lu JY, Li HQ, et al. Staging tau pathology with tau PET in Alzheimer's disease: a longitudinal study. *Transl Psychiatry*. 2021;11:483.
57. De Bastiani MA, Bellaver B, Brum WS, et al. Hippocampal GFAP-positive astrocyte responses to amyloid and tau pathologies. *Brain Behav Immun*. 2023;110:175-184.
58. Chiotis K, Johansson C, Rodriguez-Vieitez E, et al. Tracking reactive astrogliosis in autosomal dominant and sporadic Alzheimer's disease with multi-modal PET and plasma GFAP. *Mol Neurodegener*. 2023;18:60.
59. Stocker H, Beyer L, Perna L, et al. Association of plasma biomarkers, p-tau181, glial fibrillary acidic protein, and neurofilament light, with intermediate and long-term clinical Alzheimer's disease risk: results from a prospective cohort followed over 17 years. *Alzheimers Dement*. 2023;19:25-35.
60. Pereira JB, Janelidze S, Smith R, et al. Plasma GFAP is an early marker of amyloid-beta but not tau pathology in Alzheimer's disease. *Brain*. 2021;144:3505-3516.
61. Shir D, Graff-Radford J, Hofrenning EI, et al. Association of plasma glial fibrillary acidic protein (GFAP) with neuroimaging of Alzheimer's disease and vascular pathology. *Alzheimers Dement (Amst)*. 2022;14:e12291.
62. Mattsson-Carlgren N, Janelidze S, Palmqvist S, et al. Longitudinal plasma p-tau217 is increased in early stages of Alzheimer's disease. *Brain*. 2020;143:3234-3241.
63. Dore V, Doecke JD, Saad ZS, et al. Plasma p217+tau versus NAV4694 amyloid and MK6240 tau PET across the Alzheimer's continuum. *Alzheimers Dement (Amst)*. 2022;14:e12307.
64. Mendez MF. Early-onset Alzheimer disease. *Neurol Clin*. 2017;35:263-281.
65. Apostolova LG, Aisen P, Eloyan A, et al. The longitudinal early-onset Alzheimer's disease study (LEADS): framework and methodology. *Alzheimers Dement*. 2021;17:2043-2055.

SUPPORTING INFORMATION

Additional supporting information can be found online in the Supporting Information section at the end of this article.

How to cite this article: Huang K-L, Hsiao I-T, Huang C-W, et al. The Taiwan-ADNI workflow toward integrating plasma p-tau217 into prediction models for the risk of Alzheimer's disease and tau burden. *Alzheimer's Dement*. 2025;21:e14297. https://doi.org/10.1002/alz.14297